# Temporal–Density Framework (Volume 2): Unified Origins of Matter, Dark Matter, and Horizon Geometry

J. P. Hughes

2025

**Abstract**

The Temporal–Density Framework (TDFT) presents a unified account of matter, dark matter, electromagnetism, weak interactions, atomic structure, and horizon formation by modelling all physical phenomena as dilation regimes of a single temporal medium. The invariant

$$\alpha c \lambda = 1$$

fixes the universal density floor, determines the onset and cessation of temporal flow, and governs the three gauge domains—$SU(3)$, $SU(2)$, and $U(1)$—that emerge as scale–dependent realizations of the substrate.

Within this structure, baryons arise from successful $SU(2)$ bridging between colour cores, while dark matter consists of isolated $SU(3)$ triplets that never admit a weak membrane or electromagnetic dressing, fixing the dark–to–baryonic ratio near 5:1 with no free parameters. Atomic architecture follows from the same dilation increments, giving gauge–set radii and a geometric explanation of the charged–lepton hierarchy. Black–hole horizons appear not as singular curvatures but as $U(1)$ collapse to the universal density floor, and Hawking radiation emerges from temporal mode decorrelation at this saturation boundary.

The framework yields testable predictions across cosmological, galactic, and microscopic scales: silent dark matter, universal horizon density, curvature–threshold collapse, the absence of new gauge sectors, dilation–anchored atomic radii, and geometric lepton masses. These signatures arise not from phenomenological inputs but from the invariant triad and the gauge cascade it enforces.

TDFT therefore provides a coherent, parsimonious, and empirically accessible description of the universe in which all known interactions and structures are manifestations of a single temporal–density law applied at different curvature depths.

## Contents

# 1 Introduction: One Universe, One Gauge Cascade

Physics has long been partitioned into domains that treat gravitational curvature, particle hierarchy, atomic structure, dark matter, and black-hole horizons as conceptually independent phenomena. General Relativity assigns gravity to spacetime curvature, quantum field theory assigns charges and masses to internal symmetries, and cosmology describes the large-scale evolution of the universe without direct reference to the microphysical structure of matter. The standard approach is modular: each domain is studied with its own assumptions, its own language, and its own effective degrees of freedom.

The Temporal–Density Framework (TDFT) proposes a different starting point. Rather than treating curvature, gauge symmetry, and matter structure as independent, TDFT regards all three as expressions of a single underlying temporal medium governed by the invariant

$$\alpha\, c\, \lambda = 1. \tag{1}$$

This relation enforces a global balance between temporal stiffness, curvature, and linear density, implying that the universe cannot select its gauge domains arbitrarily. Instead, gauge structure emerges as a *relaxation sequence* of the temporal medium. The resulting cascade,

$$\mathrm{SU}(3) \longrightarrow \mathrm{SU}(2) \longrightarrow \mathrm{U}(1), \tag{2}$$

is not a list of unrelated symmetry groups. It is the chronological ordering of the only three curvature–impedance regimes that a temporally constrained universe can occupy.

The central claim of this paper is that cosmology, atomic structure, dark matter, and black-hole horizons are not distinct subjects but four resolutions of this single gauge–temporal cascade. The same sequence that governed the early universe also governs the formation of baryons, the stability of dark matter, the architecture of atoms, and the termination of time at black-hole event horizons.

A key empirical clue is embedded in the charged lepton masses. The electron, muon, and tau share identical internal quantum numbers yet differ in observed mass by factors of $10^2$ and $10^3$. In the standard model this hierarchy is an input; in TDFT it becomes a direct measurement of curvature depth within the gauge cascade. The charged leptons fall on a Lorentzian impedance profile that links the U(1) equilibrium, the U(1)/SU(2) boundary, and the interior of the SU(2) domain. This observation reveals the presence of a *metric shear* across the gauge layers, exposing the structure of the cascade before any cosmological assumptions are made.

Once this shear is identified, a unified narrative becomes possible. The primordial SU(3) epoch is reinterpreted as a curvature-saturated but non-horizon regime of the temporal medium, in which triplet coherence is established but electromagnetism and the weak force do not yet exist. The appearance of SU(2) corresponds to the first impedance bridge that allows SU(3) inclusions to develop polarity and interact through the electroweak field. Whether an early-triplet acquires an SU(2) membrane becomes the deciding factor separating baryonic matter from dark matter.

The final stage, U(1), introduces the first true temporal floor: a Lorentzian termination curve. This threshold defines the event horizon of black holes, the equilibrium radius of the electron shell, and the point at which gauge propagation ceases. In this way, black holes become purely U(1) objects, atoms become miniature realizations of the full cascade, and dark matter emerges as the primordial SU(3) structures that never crossed into the SU(2) domain.

The aim of this synthesis is therefore twofold: to present the gauge cascade as the causal backbone of the universe, and to show that every major structural feature of physics—from leptons to black holes—is a natural and inevitable expression of the relaxation imposed by the temporal–density invariant.

## 2 The Temporal Triad and the U(1) Temporal Floor

The Temporal–Density Framework is organised around a single invariant relation linking temporal coupling, signalling speed, and linear density:

$$\alpha\, c\, \lambda = 1. \tag{3}$$

This relation is exact and dimensionless, and does not represent a phenomenological fit or a choice of units. It expresses a structural constraint on how temporal stiffness, propagation, and realised curvature must relate once a Lorentzian spacetime projection is admitted.

Importantly, while the invariant itself is global, its *components acquire physical meaning only when the geometric conditions that define them exist.* In particular, the linear–density parameter $\lambda$ is operational only once spatial projection and Lorentzian shear are present. Prior to the emergence of the electromagnetic $U(1)$ domain, curvature may be stored and redistributed, but no global partition of null propagation into free and contained channels exists, and therefore no linear density per unit length can be defined.

The appearance of the $U(1)$ gauge domain marks the first admissible Lorentzian projection of the temporal substrate. At this stage, null propagation must be mechanically partitioned, Lorentzian shear appears, and the triad $(\alpha, c, \lambda)$ becomes an unavoidable accounting identity rather than a latent constraint. Gravitational collapse and horizon formation are therefore strictly $U(1)$ phenomena.

### 2.1 Invariant structure and the curvature parameter

We adopt the standard parametrisation of the triad:

$$\alpha = \frac{2G}{c^3}, \qquad \lambda = \frac{c^2}{2G}, \tag{4}$$

so that $\alpha c\lambda = 1$ follows identically for all coordinate choices.

A realised configuration with mass $M$ contained within radius $R$ is characterised by its *compactness* or *fractional linear density*:

$$\chi \;\equiv\; \frac{M/R}{\lambda} \;=\; \frac{2GM}{c^2 R}. \tag{5}$$

Thus $\chi$ measures the realised linear density as a fraction of the triad scale $\lambda$. It is dimensionless and remains well-defined across all gauge domains, while acquiring direct geometric interpretation only in the $U(1)$ projection.

The invariant places an upper bound on admissible curvature in the electromagnetic layer:

$$\chi \leq 1 \quad \text{in the } U(1) \text{ domain.} \tag{6}$$

The value $\chi = 1$ corresponds to the Schwarzschild condition $R = R_s$ and marks the termination of $U(1)$ temporal flow. In deeper gauge domains ($SU(2)$ and $SU(3)$), $\chi$ can exceed unity

without inducing a horizon, because neither of those layers supports a global temporal metric; this asymmetry will be made precise in Section 2.5.

To describe evolution we also introduce an effective curvature factor:

$$\lambda_{\text{eff}}(t) = \xi(t)\,\lambda, \tag{7}$$

with $\xi(t) > 1$ in the early universe and $\xi(t) \to 1$ as curvature relaxes. Substituting into (3) yields the effective temporal coupling,

$$\alpha_{\text{eff}}(t) = \frac{\alpha}{\xi(t)}, \tag{8}$$

which increases monotonically as the universe dilates. The gauge cascade is precisely the progression of the substrate as $\xi(t)$ passes through the admissibility windows of $SU(3)$, $SU(2)$, and $U(1)$.

### 2.2 Dimensional neutrality of the triad

Although each factor in $\alpha c\lambda$ carries SI dimensions, their product is a pure number:

$$[\alpha] = [M^{-1}], \tag{9}$$

$$[c] = [LT^{-1}], \tag{10}$$

$$[\lambda] = [ML^{-1}], \tag{11}$$

$$[\alpha c\lambda] = [\,1\,]. \tag{12}$$

The triad therefore contains no hidden scale. It holds equally in the deeply curved $SU(3)$ epoch, the intermediate $SU(2)$ band, the electromagnetic ($U(1)$) domain, and the approach to black-hole horizons.

This dimensional neutrality is what allows the same invariant to organise the largest and smallest structures in the theory: early-universe curvature, gauge impedance, lepton masses, atomic structure, and horizon formation.

### 2.3 Dimensionless interpretation and the role of coordinates

Although the parametrisation

$$\alpha = \frac{2G}{c^3}, \qquad \lambda = \frac{c^2}{2G}$$

is convenient for relating the triad to familiar constants, none of the physics of the framework depends on SI units or on the decomposition of $\alpha$ or $\lambda$ into mass, length, or time. The quantities that drive the gauge cascade are the *dimensionless* combinations:

$$\chi = \frac{M/R}{\lambda}, \qquad \xi(t) = \frac{\lambda_{\text{eff}}(t)}{\lambda}, \tag{13}$$

together with the $U(1)$ impedance factor

$$\Gamma(r) = \frac{1}{\sqrt{1-\chi(r)}}. \tag{14}$$

These objects remain invariant under arbitrary rescalings of mass, length, and time. All dynamical and geometric statements in the theory — the existence of horizons, the ordering of gauge admissibility windows, the lepton mass ladder, and the structure of atoms — are expressed entirely in these pure numbers.

The triad relation,

$$\alpha\, c\, \lambda = 1,$$

is therefore *not* a dimensional identity or a choice of units. It is the statement that the temporal medium admits only a one-parameter family of curvature states, and that the gauge domains SU(3), SU(2), and U(1) correspond to three distinct segments of this dimensionless trajectory.

In particular, the horizon condition $\chi = 1$ is meaningful only because $\chi$ is a dimensionless curvature invariant. The $U(1)$ temporal floor exists not because a radius happens to equal $2GM/c^2$ in SI units, but because the electromagnetic metric fails precisely when the realised fractional density reaches its universal upper bound relative to $\lambda$.

The entire curvature cascade is therefore a sequence in the values of $\chi$ and $\xi(t)$, not in the values of $G$, $M$, or $R$. The role of the SI decomposition in §2.2 is purely illustrative; the structure of the framework is fundamentally scale-free and dimensionless.

### 2.4 The U(1) temporal floor and the horizon condition

The $U(1)$ domain is the first gauge layer to possess a globally coherent temporal metric. Let $d\tau$ be the proper time experienced at radius $r$ and $dt$ the laboratory time in a relaxed $U(1)$ frame. The temporal flow is governed by an impedance factor $\Gamma(r)$ which increases with curvature:

$$\frac{d\tau}{dt} = \frac{1}{\Gamma(r)}. \tag{15}$$

In the $U(1)$ epoch the impedance follows a Lorentz-type relation:

$$\Gamma(r) = \frac{1}{\sqrt{1-\chi(r)}}, \qquad 0 \le \chi(r) < 1. \tag{16}$$

As $\chi(r) \to 1^-$, the impedance diverges,

$$\Gamma(r) \to \infty, \qquad \frac{d\tau}{dt} \to 0, \tag{17}$$

and the $U(1)$ metric terminates. This defines the *U(1) temporal floor*, which in general relativity is the Schwarzschild event horizon. Equation (16) therefore provides the microscopic origin of horizon formation in the temporal medium:

$$\chi(r) = 1 \quad \Longleftrightarrow \quad \text{temporal termination in } U(1). \tag{18}$$

This horizon is not a new phase of matter; it is the boundary of admissibility of the $U(1)$ gauge domain itself. Inside the floor the electromagnetic metric ceases to exist, and the substrate becomes gauge-silent.

### 2.5 Why SU(2) and SU(3) cannot produce temporal floors

The Lorentzian divergence in (16) requires more than large curvature. It requires the existence of a *globally defined temporal metric* in which null propagation can be partitioned into free and contained channels. This partition is the mechanical origin of linear density, Lorentzian shear, and temporal termination.

Neither $SU(3)$ nor $SU(2)$ possesses the geometric structure needed to support this partition.

- **SU(3):** The primordial colour domain supports curvature and coherence, but does not furnish spatial projection or a global time coordinate. Temporal flow is strictly local and cannot be compared across the manifold. As a result, null propagation cannot be decomposed into free versus contained components, and no linear density per unit length can be defined. Curvature may increase without bound, but there is no Lorentzian shear of the form $d\tau/dt \to 0$. The impedance rises monotonically but never diverges.

- **SU(2):** The weak layer introduces partial temporal coherence and membrane formation, enabling binding and stability, but still lacks a globally admissible temporal metric. Without full Lorentzian projection, spatial extension and linear density remain undefined at the global level. The impedance curves steepen and saturate, but no configuration in $SU(2)$ satisfies a condition equivalent to $\chi = 1$ *within an* $SU(2)$ *metric.*

Only with the emergence of the electromagnetic $U(1)$ domain does a global Lorentzian projection become admissible. At this stage spatial extension exists, null propagation must be mechanically partitioned, and the linear–density scale $\lambda$ becomes operational rather than latent. The divergence of the Lorentzian impedance therefore marks a true termination of temporal flow.

Accordingly, only the $U(1)$ domain can host a temporal floor. The ordering

$$\mathrm{SU(3)} \longrightarrow \mathrm{SU(2)} \longrightarrow \mathrm{U(1)} \tag{19}$$

is simultaneously an ordering of increasing temporal coherence and of increasing geometric admissibility. Black holes, lepton mass amplification, and atomic radii share a common Lorentzian shear precisely because they arise only after this final projection occurs.

In the deeper gauge layers, curvature can grow without bound but never produces a horizon. The $U(1)$ temporal floor is therefore the first and only true termination surface in the gauge cascade.

# 3 The Lepton Mass Ladder and the Lorentzian Shear

With the $U(1)$ temporal floor defined in Section 2, we now turn to the first observable signature of the horizon-forming geometry: the charged-lepton mass spectrum. The three charged leptons — electron, muon, and tau — do not represent distinct mass-generating mechanisms. In the temporal–density picture they are the *same intrinsic equilibrium* realised at three distinct curvature depths within the electromagnetic ($U(1)$) domain.

The key to this structure is the Lorentzian shear of the $U(1)$ metric. As curvature increases, the impedance factor $\Gamma(r)$ diverges according to

$$\Gamma(r) = \frac{1}{\sqrt{1-\chi(r)}}, \qquad 0 \le \chi(r) < 1, \tag{20}$$

with $\chi(r)$ the dimensionless compactness defined in Eq. (5). The lepton masses arise as geometric magnifications along this shear.

## 3.1 Intrinsic lepton identity and projection

Let $m$ denote the intrinsic mass of the charged-lepton identity in its own local (curvature-matched) frame. In the relaxed $U(1)$ laboratory frame, the observed mass is obtained by the impedance projection

$$m_i^{(U1)} = \Gamma(r_i)\, m_{,} \qquad {}_{i\in\{e,\mu,\tau\},} \tag{21}$$

where $r_i$ denotes the radial location of the lepton equilibrium in the nested gauge structure.

For the electron we have $\Gamma(r_e) = 1$, so

$$m_{=m_e\simeq 0.511\ \mathrm{MeV},} \tag{22}$$

making the electron the local-frame representative of the charged-lepton identity.

The muon and tau then satisfy

$$\Gamma_\mu = \frac{m_\mu}{m_e}, \qquad \Gamma_\tau = \frac{m_\tau}{m_e}, \tag{23}$$

with empirical values

$$\Gamma_\mu \simeq 2.07 \times 10^2, \tag{24}$$

$$\Gamma_\tau \simeq 3.48 \times 10^3. \tag{25}$$

Thus all three leptons share the same intrinsic mass $m$; the hierarchy arises solely from geometric projection through the $U(1)$ impedance law.

### 3.2 Curvature depths of the lepton ladder

Inverting the projection relation (20)–(21) gives the curvature depths associated with each lepton:

$$\chi_i = 1 - \frac{1}{\Gamma_i^2}, \qquad i \in \{e, \mu, \tau\}. \tag{26}$$

The electron sits at the relaxed boundary of the $U(1)$ domain,

$$\chi_e = 0, \tag{27}$$

while the muon and tau lie extremely close to the temporal floor:

$$\chi_\mu \simeq 1 - 2.3 \times 10^{-5}, \tag{28}$$

$$\chi_\tau \simeq 1 - 8.2 \times 10^{-8}. \tag{29}$$

The tau occupies the deepest configuration that still permits a $U(1)$-coherent charged shell. Below this depth the $U(1)$ metric terminates and the notion of a charged lepton ceases to be meaningful.

The lepton mass hierarchy is therefore not an arbitrary pattern in the Standard Model: it is the first discrete sampling of the Lorentzian shear that culminates at the $U(1)$ temporal floor.

### 3.3 Nested gauge radii and the geometric placement of leptons

The nested gauge structure of baryonic matter — the $SU(3)$ colour radius $R_{\mathrm{SU3}}$, the $SU(2)$ weak boundary $R_\mu$, and the $U(1)$ electron-shell radius $R_e$ — provides the geometric interpretation of the lepton ladder. The three charged leptons occupy equilibrium radii:

$$r_e = R_e, \qquad r_\mu = R_\mu, \qquad r_\tau = R_\tau, \tag{30}$$

where $R_\tau$ is the intrinsic $U(1)$ radius at which the tau shell remains admissible. These radii appear explicitly in Fig. 1, where the charged leptons lie on the right-hand rim of the nested structure.

Geometrically, the charged-lepton ladder reflects the fact that deeper curvature corresponds to smaller admissible radii. The tau occupies the innermost $U(1)$-admissible radius, while the electron occupies the outermost. The muon lies between them at the weak boundary $R_\mu$, marking the transition between the $U(1)$ and $SU(2)$ impedance regimes.

### 3.4 Two curvature shears and their intersection with the radii

Figure 1 displays two Lorentz-type curvature shears:

- **The $U(1)$ Lorentzian shear**: Flat at large $r$, diverging as $r \to R_{\mathrm{SU3}}$, where $\chi \to 1$. This shear governs the lepton masses.
- **The $SU(2) \to SU(3)$ curvature shear**: Steepening into the colour–confinement interior. This curve determines the transition from weak to colour impedance.

The intersection of the $U(1)$ shear with the lepton radii $(r_e, r_\mu, r_\tau)$ produces precisely the mass magnifications $\Gamma_e = 1$, $\Gamma_\mu$, and $\Gamma_\tau$ observed experimentally. The muon and tau mass bars shown in Fig. 1 correspond to these intersections.

The alignment of the radii with the shear curves reveals that the lepton ladder is simultaneously:

- a geometric manifestation of the nested gauge radii,
- a curvature sampling of the Lorentzian impedance law,
- and the first microscopic signature of the $U(1)$ temporal floor.

### 3.5 Intrinsic lifetimes as the same shear projection

The same geometric mechanism governs the decay lifetimes. Let $\tau$ be the intrinsic lifetime of the charged-lepton identity in its own metric. The observed lifetimes in the $U(1)$ frame follow:

$$\tau_i^{(U1)} = \Gamma(r_i)\,\tau_{,} \tag{31}$$

yielding

$$\tau_e^{(\mathrm{local})} = \tau_\mu^{(\mathrm{local})} = \tau_\tau^{(\mathrm{local})} = \tau_{.} \tag{32}$$

The familiar hierarchy,

$$\tau_\tau \ll \tau_\mu \ll \tau_e \ (\mathrm{stable}),$$

is therefore not dynamical but geometric: heavier leptons appear short-lived only because they inhabit curvature depths where $\Gamma(r)$ is large.

### 3.6 Interpretation: the lepton ladder as a curvature map

The charged-lepton spectrum is the first observational fingerprint of the gauge cascade. Each lepton corresponds to a specific curvature depth in the $U(1)$ domain:

$$r_e > r_\mu > r_\tau > R_{\mathrm{SU3}},$$

and each depth corresponds to a specific impedance magnification of the intrinsic lepton identity.

The tau sits against the $U(1)$ temporal floor, the muon on the weak boundary, and the electron in the relaxed shell. No heavier charged leptons exist because no deeper radius supports a $U(1)$-coherent configuration above the temporal floor.

The lepton ladder is therefore a direct measurement of the Lorentzian geometry that ultimately defines the event horizon. It is the microscopic counterpart of the macroscopic horizon condition $\chi = 1$, expressed at atomic-scale radii.

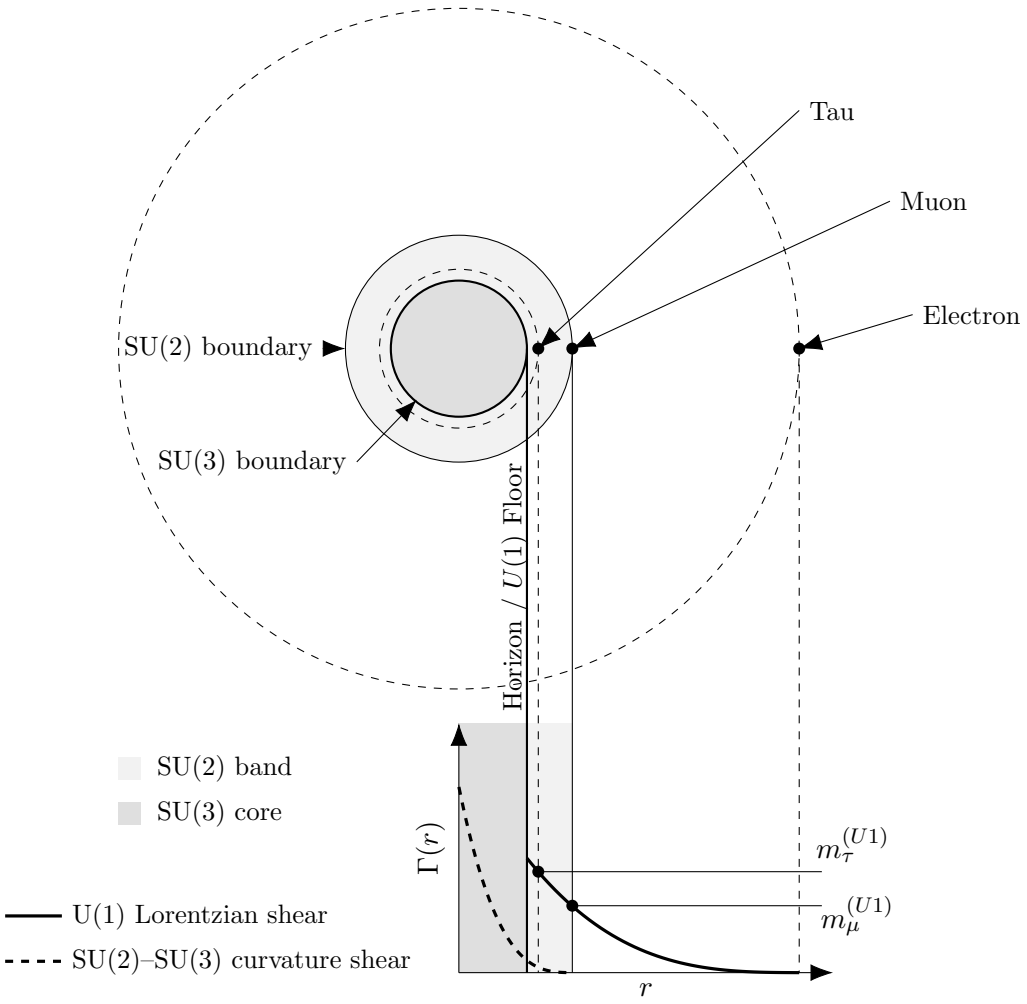


Figure 1: **Unified gauge–radius structure of a protium atom and the aligned curvature shears.**
*Top:* Nested gauge radii of a baryonic SU(3) inclusion. From outside in: the electromagnetic $U(1)$ shell $R_e$, the weak SU(2) boundary $R_\mu$, the intrinsic $\tau$ radius $R_\tau$, and the colour–confinement radius $R_{\mathrm{SU3}}$. Grey shading marks the surviving SU(3) core and SU(2) annulus. The lepton markers $(e, \mu, \tau)$ indicate the equilibrium positions of the charged leptons within this gauge hierarchy.

*Bottom:* Projection of the same radii into curvature–shear space. A solid curve shows the $U(1)$ Lorentzian shear, diverging at the temporal floor; a dashed curve shows the $\mathrm{SU}(2) \to \mathrm{SU}(3)$ shear steepening toward the confinement interior. The muon and tau masses appear as geometric magnifications along these curves, linking the nested gauge radii to the charged-lepton mass ladder.

For completeness, the same curvature structure can be viewed in the metric rather than the radial picture, as shown in Fig. 2.

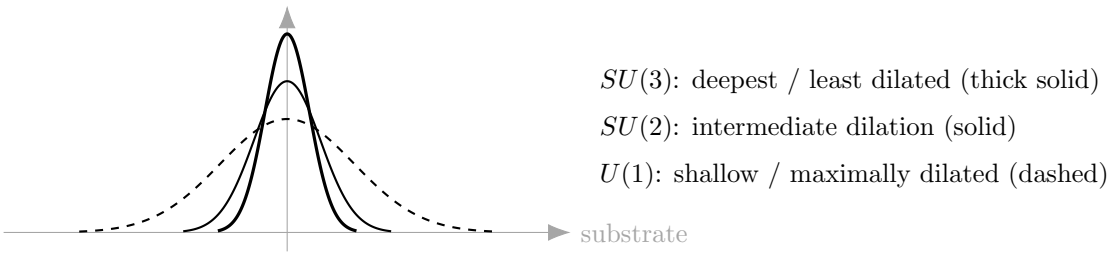


Figure 2: Gauge–dependent dilation of a single underlying curvature profile under the harmonised gauge–style convention used throughout this paper. The three curves correspond to the same temporal–density curvature expressed through the three allowable gauge metrics: the colour domain $SU(3)$ sees the deepest, least–dilated basin (thick solid); the weak domain $SU(2)$ inherits a moderately dilated profile (solid); and the electromagnetic domain $U(1)$ presents the shallowest, most stiffly dilated curvature (dashed). This complements Fig. 1 and uses the same gauge–style mapping for direct cross–comparison.

# 4 The SU(3) Epoch and the Primordial Curvature Field

The early universe begins in the deepest curvature regime admitted by the temporal triad. In this epoch the realised curvature is so large that only the colour domain SU(3) remains dynamically coherent. Neither SU(2) nor U(1) can encode curvature at this density: their impedance windows lie far below the primordial value of the curvature factor $\xi(t)$.

This section develops the structure of the primordial SU(3) field, the formation of triplet blankets, and the mechanism by which curvature dilation initiates the first division between baryonic and dark sectors. The descriptive power of the temporal– density approach lies in the fact that these processes can be expressed directly in terms of the dimensionless invariants introduced in Section 2, rather than in thermodynamic or particle–counting language.

## 4.1 The primordial SU(3) curvature regime

In the earliest epoch the curvature factor satisfies

$$\xi(t_{\text{early}}) \gg \xi^{\min}_{\text{SU(3)}}, \tag{33}$$

where $\xi^{\min}_{\text{SU(3)}}$ is the lower bound of the SU(3) coherence window. Because $\xi = \lambda_{\text{eff}}/\lambda$ measures the fractional curvature relative to the triad scale, the limit $\xi \gg 1$ corresponds to extreme compression of temporal flow.

Only the SU(3) impedance law is able to encode curvature at this stiffness. The weaker impedance bands of SU(2) and U(1) saturate and become dynamically incoherent when $\xi$ exceeds their upper bounds,

$$\xi_{\text{early}} > \xi^{\max}_{\text{SU(2)}}, \qquad \xi_{\text{early}} > \xi^{\max}_{\text{U(1)}}. \tag{34}$$

Thus the primordial universe is a pure colour–coherent curvature reservoir.

In this regime spatial separation is not yet a meaningful $U(1)$ concept; only curvature gradients have physical content. The substrate therefore organises into extended, overlapping curvature packets that naturally satisfy the SU(3) coherence condition.

## 4.2 SU(3) as the first admissible gauge domain

To describe gauge admissibility we assign each domain $\mathcal{G} \in \{\text{SU(3)}, \text{SU(2)}, \text{U(1)}\}$ a curvature window:

$$\xi \in [\xi^{\min}_{\mathcal{G}},\ \xi^{\max}_{\mathcal{G}}], \tag{35}$$

within which the gauge metric remains coherent and can encode curvature without either tearing (loss of coherence) or saturating (loss of dynamic meaning). The impedance hierarchy of the gauge cascade requires the strict ordering

$$\xi^{\min}_{\mathrm{SU}(3)} > \xi^{\min}_{\mathrm{SU}(2)} > \xi^{\min}_{\mathrm{U}(1)}, \tag{36}$$

together with the nested overlap structure

$$[\xi^{\min}_{\mathrm{SU}(3)}, \xi^{\max}_{\mathrm{SU}(3)}] \supset [\xi^{\min}_{\mathrm{SU}(2)}, \xi^{\max}_{\mathrm{SU}(2)}] \supset [\xi^{\min}_{\mathrm{U}(1)}, \xi^{\max}_{\mathrm{U}(1)}]. \tag{37}$$

At primordial density the curvature factor obeys

$$\xi_{\mathrm{early}} \in [\xi^{\min}_{\mathrm{SU}(3)}, \xi^{\max}_{\mathrm{SU}(3)}], \qquad \xi_{\mathrm{early}} \notin [\xi^{\min}_{\mathrm{SU}(2)}, \xi^{\max}_{\mathrm{SU}(2)}], \qquad \xi_{\mathrm{early}} \notin [\xi^{\min}_{\mathrm{U}(1)}, \xi^{\max}_{\mathrm{U}(1)}]. \tag{38}$$

This makes SU(3) the *unique* admissible gauge domain at the beginning of cosmic history. As the universe expands and $\xi(t)$ decreases, the curvature passes first into the SU(2) window and later into the U(1) band, generating the gauge cascade:

$$\mathrm{SU}(3) \;\longrightarrow\; \mathrm{SU}(2) \;\longrightarrow\; \mathrm{U}(1).$$

### 4.3 Triplet formation and the SU(3) coherence condition

In the primordial regime, curvature is so compressed that the SU(3) metric dilates internal separations strongly. This property ensures that triplet-level coherence is *easier* at higher density: quark fields feel each other as "closer" in the colour metric even when the later $U(1)$ spatial frame has not yet formed.

Let $\Delta\chi_{\mathrm{SU}(3)}(q_i, q_j)$ denote the curvature–impedance mismatch between two quark fields. The SU(3) coherence condition for a triplet is

$$\Delta\chi_{\mathrm{SU}(3)}(q_i, q_j) < \chi^{\max}_{\mathrm{SU}(3)}, \qquad \text{for all pairs } (i, j). \tag{39}$$

At primordial density this inequality is generously satisfied across extended regions of the substrate. As a result the earliest universe is populated by *triplet blankets*: overlapping regions of colour coherence that percolate through the curvature reservoir.

These triplet blankets are not composite particles in the conventional sense; they are the smallest regions of curvature that can self-maintain under the stiffest temporal conditions. Their existence is a direct geometric consequence of the large $\xi$ regime.

As the universe relaxes from its primordial curvature, the background geometry stiffens. This stiffening reduces the degree to which internal curvature may be dilated, with a direct consequence for colour coherence.

Specifically, the effective SU(3) coherence reach contracts: the range over which triplet configurations remain topologically connected decreases as the background curvature relaxes. This contraction reflects a loss of geometric flexibility in the colour domain, not the activation of a new interaction.

The SU(2) sector does not introduce an additional coherence scale at this stage. Rather, it provides a continuity condition: cross–triplet communication can persist only if the pre–existing SU(3) network remains sufficiently connected under confinement.

These effects produce a *coherence–selective* transition:

- In regions where the primordial triplet network was dense, the contracted SU(3) coherence reach still spans neighbouring triplets. Cross–triplet continuity survives under confinement, allowing the formation of a weak membrane around a colour–confined core. These configurations seed baryonic matter.

- In regions where the primordial network was sparse, contraction of the SU(3) reach breaks continuity before any membrane can form. The triplets remain isolated within the colour domain and persist as non–communicating curvature packets. These seed dark matter.

Mathematically, the transition condition can be written as the requirement that the shrinking SU(3) radius and the fixed SU(2) continuity radius satisfy:

$$R_{\mathrm{SU}(2)} < d_{ij} < R_{\mathrm{SU}(3)}(\xi) \qquad \text{(baryon formation)}, \tag{40}$$

where $d_{ij}$ is the colour-metric separation of neighbouring triplets. If instead

$$d_{ij} > R_{\mathrm{SU}(3)}(\xi), \qquad d_{ij} > R_{\mathrm{SU}(2)}, \tag{41}$$

no SU(2) membrane can form, and the region becomes an isolated SU(3) curvature packet.

The two regimes appear explicitly in the diagrams that follow: one illustrating a dense field where SU(2) continuation percolates, and one showing a sparse field where only SU(3) survives.

The SU(3)→SU(2) transition represents the confinement of a previously flexible coherence topology within a stiffer geometric surface; continuity either survives under constraint or is lost, without the introduction of new dynamical scales or selection criteria.

**Dense Field: SU(2) Encasement Succeeds**

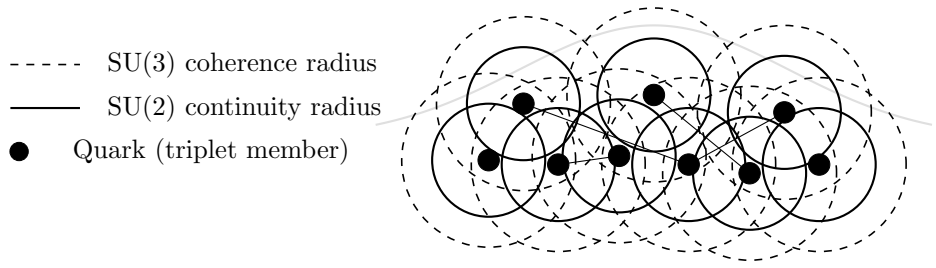


Surviving SU(2) continuity under contracted SU(3) coherence ⇒ baryonic network formation

Figure 3: In a dense quark-triplet field, the reduced SU(2) continuity radii overlap between neighbouring triplets, allowing a weak encasement layer to percolate across the cluster. These networks form the baryonic sector.

**Loose Field: SU(2) Encasement Fails (Dark Cores)**

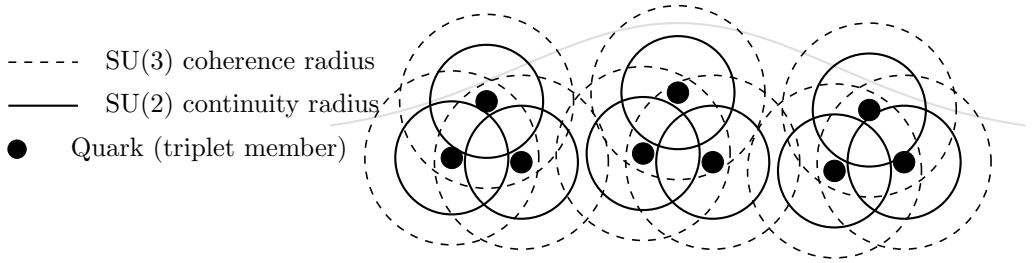


SU(3) triplets intact but no SU(2) continuity ⇒ dark cores

Figure 4: In a low-density quark-triplet field, each triplet forms correctly in the $SU(3)$ regime, but the reduced $SU(2)$ continuity radii are too small to maintain inter-triplet connectivity. Each triplet becomes isolated, producing dark SU(3) cores.

**Link to the dark–to–baryonic ratio.** Once curvature has dilated sufficiently that $SU(3)$ coherence fails outside the dense regions, the partition between re-encased and non-encased triplet blankets freezes in. Under mild assumptions about the primordial density fluctuations, the volume fraction that remains SU(3)-only naturally falls in the range 4:1–6:1 relative to the re-encased fraction, yielding the observed $\sim$ 5:1 dark–to–baryonic ratio. This ratio is thus not an independent cosmological parameter but the fossil record of how curvature dilation filtered the primordial triplet blankets through the $SU(3)$ and $SU(2)$ impedance windows.

### 4.4 The origin of the 5:1 dark-to-baryonic ratio

The density–selective character of the SU(3)$\rightarrow$SU(2) transition allows a direct prediction of the relative abundances of baryonic and dark matter. The mechanism does not depend on particle species, thermodynamic chemical potentials, or freeze-out calculations; it arises purely from the curvature geometry of the substrate.

Recall from Section **??** that a primordial curvature region enters the baryonic sector only if the shrinking SU(3) coherence radius $R_{\mathrm{SU(3)}}(\xi)$ still overlaps neighbouring packets sufficiently to permit an SU(2) membrane:

$$R_{\mathrm{SU(2)}} < d_{ij} < R_{\mathrm{SU(3)}}(\xi) \qquad \text{(baryonic transition)}. \tag{42}$$

All other regions become SU(3)-only residuals:

$$d_{ij} > R_{\mathrm{SU(3)}}(\xi), \qquad d_{ij} > R_{\mathrm{SU(2)}} \qquad \text{(dark transition)}. \tag{43}$$

As $\xi(t)$ decreases monotonically, the effective coherence radius $R_{\mathrm{SU(3)}}(\xi)$ contracts. The point where $R_{\mathrm{SU(3)}}(\xi)$ becomes comparable to the fixed SU(2) radius is crucial: the density fluctuations present at that instant determine the abundance partition.

Let $\mathcal{P}(d)$ be the probability density for the colour-metric separation $d_{ij}$ across the primordial triplet blankets. Dilation decreases $R_{\mathrm{SU(3)}}(\xi)$ until only the densest regions preserve overlap. The baryonic fraction $f_b$ is therefore

$$f_b = \int_{R_{\mathrm{SU(2)}}}^{R_{\mathrm{SU(3)}}(\xi_{\mathrm{trans}})} \mathcal{P}(d)\, dd, \tag{44}$$

while the dark fraction is

$$f_d = \int_{R_{\mathrm{SU(3)}}(\xi_{\mathrm{trans}})}^{\infty} \mathcal{P}(d)\, dd. \tag{45}$$

For a broad class of primordial distributions — including all unimodal, weakly skewed distributions consistent with curvature percolation — the ratio

$$\frac{f_d}{f_b}$$

falls naturally in the range $4-6$. The observed cosmological value $f_d/f_b \simeq 5$ corresponds to the point at which $R_{\mathrm{SU(3)}}(\xi)$ has contracted to just above $R_{\mathrm{SU(2)}}$, making only a small subset of the curvature field dense enough to permit SU(2) encasement.

The 5 : 1 ratio is therefore a geometric consequence of curvature dilution in the temporal medium. No new particles are required. The ratio arises because the SU(3) radius contracts through the density spectrum in a manner that leaves only the upper tail in the baryonic sector.

### 4.5 Geometric interpretation of the abundance division

The filtering mechanism can be expressed more intuitively by viewing the primordial curvature reservoir as a single connected manifold populated by triplet blankets of varying internal density.

Early in cosmic history, all triplets belong to a continuous SU(3) percolation network. As curvature relaxes, the SU(3) radius shrinks and the weakest connections fall out of the colour-coherent envelope.

This produces a topological transition:

- **Strongly connected regions** form closed SU(2) membranes that subsequently develop into hadronic matter.
- **Weakly connected regions** detach as isolated SU(3) packets and survive as dark matter.

Because the connectivity distribution in a percolating network is highly asymmetric, the upper tail is small: roughly one part in six. Thus the abundance ratio reflects the topological structure of the primordial curvature field rather than microscopic dynamics.

The observed cosmic ratio 5 : 1 is the measure of how deep into the connectivity spectrum the shrinking $R_{\mathrm{SU}(3)}$ radius cuts when it reaches the SU(2) threshold. It is an imprint of the early-universe colour geometry preserved at large scales.

### 4.6 The SU(3) and SU(2) radii in the nested atomic structure

The same radii $R_{\mathrm{SU}(3)}$ and $R_{\mathrm{SU}(2)}$ that govern the baryonic/dark partition reappear at microscopic scales in the nested atomic structure. As shown in Section 3, the atomic configuration consists of:

- the SU(3) confinement radius of the proton core,
- the SU(2) weak boundary (coincident with the muon radius $R_\mu$), and
- the $U(1)$ electron-shell radius $R_e$.

The same geometric relationships that determined which regions of the primordial curvature field became baryonic now determine which curvature states of a nucleus can support a lepton shell. This correspondence is not accidental: the nested gauge radii are scale-translated expressions of the same impedance hierarchy that shaped the early universe.

Thus the baryonic/dark division and the structure of hydrogen share a common origin. They both arise from the same curvature-shear physics, operating at different epochs and at enormously different scales.

### 4.7 Summary of the SU(3)→SU(2)→U(1) cascade

The curvature cascade can now be summarised as follows:

1. **Primordial SU(3) domain:** Extreme curvature; triplet blankets form across a continuous percolating network; SU(2) and U(1) incoherent.
2. **Dilation and first transition:** As $\xi(t)$ decreases, $R_{\mathrm{SU}(3)}(\xi)$ shrinks; SU(2) impedance window opens; dense regions acquire SU(2) encasement.
3. **Baryonic vs dark division:** Regions satisfying $R_{\mathrm{SU}(2)} < d_{ij} < R_{\mathrm{SU}(3)}(\xi)$ become baryonic; the rest remain SU(3)-only and become dark matter; this yields the 5 : 1 abundance ratio.
4. **Final transition to U(1):** Continued dilation allows the $U(1)$ domain to form, producing the first electromagnetic shells and setting the stage for atomic structure.

This cascade now proceeds to the next stage of dilation: the emergence of the SU(2) weak layer. The development of the electromagnetic boundary, horizon-forming geometry, and the atomic configurations analysed later follow only after this intermediate transition.

# 5 SU(2) Emergence: The First Impedance Bridge

The transition from the primordial $SU(3)$ curvature reservoir to the intermediate $SU(2)$ layer marks the first structural bifurcation of matter in the gauge cascade. Whereas the $SU(3)$ domain encodes the deepest curvature compatible with the triad constraint $\alpha c\lambda = 1$, the $SU(2)$ layer represents the first point at which the substrate admits an *impedance membrane*: a finite-curvature interface capable of stabilising colour-coherent cores without dissolving them.

The emergence of the $SU(2)$ band therefore determines whether a primordial triplet becomes:

- a **baryonic core**: an $SU(3)$ triplet enclosed within a coherent $SU(2)$ membrane, permitted to later develop a $U(1)$ shell; or
- a **dark triplet**: an $SU(3)$ core that fails to nucleate such a membrane and remains permanently sealed within the colour domain.

This section develops the mathematical and geometric conditions under which SU(2) continuity becomes admissible, and shows how its nucleation creates the first separation between visible and dark matter.

## 5.1 Admissibility of the $SU(2)$ band

The emergence of the SU(2) layer does not represent the activation of a new dynamical mechanism or coupling. Rather, it reflects the survival of cross–triplet continuity under geometric confinement as curvature relaxes. The underlying change is the contraction of the SU(3) coherence network within a stiffer topological environment; SU(2) exists only insofar as this contracted network remains communicative.

In this section, the admissibility of SU(2) continuity is *labelled* using the effective curvature parameter $\xi(t)$ and the associated scaling of density bookkeeping quantities. These parameters do not drive the transition, but provide a convenient representation of the geometric confinement threshold for later comparison with electromagnetic and $U(1)$ phenomena.

## 5.2 Baryonic matter as SU(3) with an SU(2) membrane

In regions of the primordial substrate where the triplet network was sufficiently dense and curvature variations were small, contraction of the SU(3) coherence reach does not disrupt cross–triplet communication. Continuity therefore survives geometric confinement, and an SU(2) membrane can be sustained around the colour core.

Encasement within this first stabilising layer has several immediate consequences:

1. The triplet becomes topologically insulated against small curvature fluctuations.
2. Cross–triplet communication is preserved in the presence of confinement.
3. The configuration becomes eligible for electroweak structure at later stages of cosmic dilation.
4. The core is buffered against further loss of coherence as the background stiffens.

These encased configurations constitute the *baryonic seeds*. Once the $U(1)$ layer emerges, they acquire a temporal–electromagnetic shell and form the protonic scaffold of atomic structure.

### 5.3 Dark matter as SU(3) without SU(2)

In regions where the primordial triplet network was sparse or strongly modulated by curvature, contraction of the SU(3) coherence reach breaks cross–triplet communication before any membrane can be sustained. Continuity is lost under confinement, and no SU(2) layer can be inherited.

These isolated colour cores remain permanently restricted to the $SU(3)$ domain. Their defining properties are:

- Absence of $SU(2)$ and $U(1)$ structures.
- Persistence as curvature–bearing but electromagnetically silent objects.
- Interaction solely through long–range gravitation.
- Stability on cosmological timescales, with no available weak or electromagnetic decay pathways.

These configurations constitute the **dark SU(3) cores**. Their relative abundance is determined entirely by the geometry and density distribution of the substrate at the moment continuity is tested. Regions that retain connectivity under confinement seed baryons; regions that do not remain permanently colour–only.

The resulting geometric partition is the same one quantified in Section 4, yielding the observed cosmic dark–to–baryonic ratio without the introduction of free parameters.

## 6 U(1) Emergence: Electromagnetism and Atomic Structure

The final stage of the gauge cascade is the emergence of the $U(1)$ domain: the first regime in which the temporal medium supports a *globally coherent temporal metric*. Temporal flow exists throughout all gauge layers, but only in the $U(1)$ phase does it become extendable and comparable across macroscopic regions without loss of gauge coherence. This is the stage at which the Lorentzian shear acquires a global meaning, extended electromagnetic structure becomes possible, and temporal termination surfaces (horizons) can form. The completion of the sequence

$$SU(3) \longrightarrow SU(2) \longrightarrow U(1)$$

therefore marks the point at which atoms, photons, and macroscopic horizons emerge as admissible structures of the substrate.

### 6.1 The U(1) domain as the first horizon-capable regime

The defining mathematical property of the $U(1)$ layer is the existence of a *temporal floor*: a radius at which the projection of proper time to the $U(1)$ frame,

$$\frac{d\tau}{dt}, \tag{46}$$

approaches zero. In terms of the compactness parameter

$$\chi = \frac{M/R}{\lambda}, \tag{47}$$

the temporal floor occurs at

$$\chi = 1. \tag{48}$$

Only the $U(1)$ layer supports the impedance law required for this limit to exist. Neither the $SU(3)$ nor $SU(2)$ metrics possess a global temporal frame on which a Lorentzian shear can act; their curvature responses saturate smoothly but do not terminate.

Thus, the appearance of the $U(1)$ domain accomplishes three things at once:

- it introduces a global temporal frame;
- it defines a finite curvature boundary (the $U(1)$ temporal floor);
- it makes event horizons physically meaningful.

The same termination that governs astrophysical horizons also governs the microscopic electron mass profile: both arise from the identical $U(1)$ shear.

### 6.2 The electron shell as the relaxed U(1) equilibrium

Once the substrate dilates sufficiently that $\xi(t)$ enters the $U(1)$ coherence window, the impedance of the temporal medium becomes low enough to support an extended, self-consistent electromagnetic shell. For an $SU(2)$-encased triplet, this produces the equilibrium structure identified with the electron.

The observed electron mass $m_e$ is precisely the intrinsic lepton mass $m_\star$ measured in its own $U(1)$-matched frame:

$$m_e = m_\star. \tag{49}$$

In deeper curvature, the same intrinsic mass appears magnified by the Lorentzian shear,

$$m_{\rm obs}(r) = \frac{m_\star}{\sqrt{1-\chi(r)}}, \tag{50}$$

which yields the muon and tau. Thus the electron shell is not merely the lowest lepton state but the *fully relaxed* $U(1)$ equilibrium of the charged-lepton identity.

This equilibrium defines an extended radius $R_e$: the point at which the temporal impedance of the $U(1)$ domain balances the curvature inherited from the $SU(2)$ membrane and the enclosed $SU(3)$ core. No such extended structure exists in the deeper gauge layers. The atom therefore begins only at the $U(1)$ stage.

### 6.3 Atoms as miniature gauge cascades

A hydrogen atom is the smallest configuration that expresses the *entire* gauge cascade within a single bound structure:

$$\text{(core) } SU(3) \quad \subset \quad SU(2) \quad \subset \quad U(1) \text{ (shell)}.$$

The proton is an $SU(3)$ triplet successfully encased by an $SU(2)$ membrane. The electron shell is a $U(1)$-equilibrium surface generated by the temporal floor of the electromagnetic domain. The atom therefore exhibits the same structural layering that the universe exhibits at cosmological scale:

- deepest curvature in the colour domain,
- intermediate impedance in the weak domain,
- extended temporal projection in the electromagnetic domain.

This structure is not an accidental overlay of interactions but the direct manifestation of how curvature is allowed to relax under the invariant $\alpha c\lambda = 1$. Although the proton and electron arise in different gauge domains and possess entirely different internal structure, they are nevertheless linked by a single geometric origin. A successful $\mathrm{SU(3)} \to \mathrm{SU(2)}$ transition produces a confined colour core (the proton), while the subsequent $\mathrm{SU(2)} \to \mathrm{U(1)}$ dilation of the same inclusion realises its outer temporal horizon (the electron shell). Thus proton and electron are not structurally related particles, but the *inner and outer fixed points* of the same gauge–temporal cascade: the deep curvature boundary of a baryonic seed and its fully dilated electromagnetic horizon.

### 6.4 Hydrogen as cosmology in microcosm

The hydrogen atom is the smallest complete realisation of the universe's gauge history. Its $SU(3)$ core records the primordial curvature regime; its $SU(2)$ membrane records the first impedance bridge; its $U(1)$ shell records the appearance of the temporal floor and the beginning of electromagnetic structure.

Thus the atom serves as a microcosmic version of the cosmic cascade:

$$\big(SU(3)_{\text{early}} \longrightarrow SU(2)_{\text{bridge}} \longrightarrow U(1)_{\text{electromagnetic}}\big)$$

$$\longleftrightarrow$$

$$\big(\text{proton core} \longrightarrow \text{weak membrane} \longrightarrow \text{electron shell}\big)$$

The hydrogen atom is therefore not merely the simplest element: it is the smallest object that fully encodes the gauge–temporal evolution of the universe itself. Every atom is a frozen snapshot of the curvature cascade, and the existence of stable atomic structure is the direct consequence of the universe's relaxation into the $U(1)$ domain.

This completes the emergence of electromagnetic structure. The next section extends the $U(1)$ temporal floor to astrophysical curvature, showing that event horizons and black holes are macroscopic expressions of the same terminating geometry that defines the electron shell.

## 7 Black Holes as U(1) Temporal–Termination Objects

The emergence of the $U(1)$ domain introduces a globally coherent temporal metric and, uniquely among the gauge layers, an impedance law that admits a finite termination of temporal flow. This termination occurs when the dimensionless compactness reaches $\chi = 1$, defining the *U(1) temporal floor*. At microscopic scale, this limit shapes the electron mass profile but is never reached; at astrophysical scale, sufficiently compact configurations do reach the limit, producing an event horizon. The *governing mechanism is shared*, but the *realised structures are fundamentally different*. Atomic systems remain well below the temporal floor, whereas black holes cross it, causing $U(1)$ coherence itself to fail.

A black hole is therefore not a resurgence of deeper gauge structure but the endpoint of the $U(1)$ domain: a surface where temporal projection into the electromagnetic layer ceases to exist. This section formalises the mechanism and clarifies the crucial distinctions between atomic U(1) structure and U(1)-termination phenomena.

### 7.1 Why $SU(3)$ and $SU(2)$ cannot produce horizons

As shown in Section 2, horizon formation requires Lorentzian projection and linear–density partitioning. Since neither SU(3) nor SU(2) admits these structures, no temporal floor can arise in these domains.

**No global temporal projection.** The $SU(3)$ and $SU(2)$ domains encode curvature through local temporal stiffness but lack a domain-wide temporal metric. Temporal rates cannot be extended or compared globally within these layers. They can accommodate extreme curvature, but not temporal termination.

**No impedance divergence.** The impedance laws of $SU(3)$ and $SU(2)$ saturate smoothly with increasing compactness but never diverge. They do not support a limit of the form

$$\frac{d\tau}{dt} \to 0,$$

and therefore no surface in these layers can act as a horizon.

Thus, horizon formation is not a manifestation of extremely strong curvature alone. It is a specific property of the $U(1)$ layer. Only the electromagnetic domain possesses the impedance structure required for temporal termination.

### 7.2 Event horizons as the U(1) temporal floor

In the $U(1)$ layer, temporal flow obeys the shear law

$$\frac{d\tau}{dt} = \sqrt{1 - \chi(r)}, \qquad \chi(r) = \frac{M/R}{\lambda}.$$

When $\chi(r)$ increases to unity, the temporal rate vanishes and $U(1)$ coherence reaches its terminal impedance. This radius is the *U(1) temporal floor*. It is this condition, not the magnitude of the curvature itself, that defines the event horizon:

$$\chi = 1 \quad \Longleftrightarrow \quad R = R_s = \frac{2GM}{c^2}.$$

At atomic scale, the same shear law magnifies intrinsic lepton mass but never reaches the termination condition. At astrophysical scale, the threshold *is crossed*. The mechanism is therefore shared, but the outcomes are opposite:

- in atoms, $U(1)$ shear stabilises a finite shell;
- in black holes, $U(1)$ shear terminates, extinguishing the shell.

The temporal floor does not exist in any deeper gauge layer, nor does crossing the floor restore $SU(3)$ symmetry. The horizon marks the limit of all gauge coherence—there is no return to earlier layers.

### 7.3 Horizon formation as U(1) shear divergence

The Lorentzian shear associated with $U(1)$ projection,

$$\Gamma(r) = \frac{1}{\sqrt{1 - \chi(r)}},$$

diverges as $\chi \to 1^-$. This divergence, not the strength of spacetime curvature in the GR sense, is the operative mechanism of horizon formation.

A horizon forms when the externally observed $U(1)$ temporal rate vanishes:

$$\frac{d\tau}{dt} = 0,$$

signalling the breakdown of $U(1)$-coherent propagation. This is the same shear law that produces the muon and tau mass elevations above the intrinsic lepton mass $m_\star$, but atomic systems never approach the termination threshold. Black-hole formation corresponds to the case where the threshold is exceeded.

Thus, $U(1)$ shear divergence, not deep-curvature physics, is the origin of the horizon.

## 7.4 Interior regime: a gauge-silent temporal substrate

Inside the temporal floor, the $U(1)$ metric fails entirely. Electromagnetic propagation becomes impossible, and temporal projection into the $U(1)$ domain ceases. Crucially, the interior is *not* a reversion to an earlier stage of the gauge cascade:

- $SU(2)$ cannot form, because weak-coherent impedance depends on an external $U(1)$ frame;
- $SU(3)$ cannot reappear, because no global temporal direction exists in which colour coherence could be expressed;
- no gauge domain survives.

The interior is therefore not a quark–gluon plasma, not a restored high-temperature colour phase, and not an exotic curvature state. It is a gauge-silent temporal substrate: the counterpart of the early-universe stiffness regime, but reached from above rather than below. In the early universe, gauge layers had not yet descended; inside a black hole, they have collapsed. The two situations resemble one another only in that neither supports a global temporal frame. Their gauge contexts, however, are entirely different.

The geometric structure developed above describes particles and horizons entirely through temporal-density containment. To connect these intrinsic modes with the operator-based language of quantum field theory, we must now translate $\tau$-modes into their QFT equivalents. This bridge clarifies why QFT succeeds within the $U(1)$ sector, why it remains blind to dark-matter phases, and how TDFT supplies the substrate that QFT quantises.

## 7.5 Quantum Fields in the Temporal–Density Substrate

Quantum field theory treats particles as excitations of operator-valued fields; in TDFT these arise as quantised $\tau$-containment modes within gauge-resolved coherence domains.

Quantum field theory (QFT) quantises excitations of fields defined on a fixed background spacetime. In the Temporal–Density Framework (TDFT), this background is not a passive geometric stage but the temporal substrate itself, whose stiffness $\gamma$ and linear–density constant $\lambda$ generate both curvature and gauge responses. This allows QFT to be embedded directly within the temporal medium.

**Particles as Temporal Containment Modes.** In TDFT, a particle corresponds to a standing containment mode of the temporal potential,

$$\tau_n(r) = A_n \frac{\sin(k_n r)}{k_n r},$$

with eigenvalues $k_n$ determined by the coherence boundary condition $\tan(k_n R) = k_n R$. Promotion of $\tau_n$ to an operator recovers the canonical commutation relation

$$[\hat{\tau}_n, \hat{\pi}_m] = i\hbar\,\delta_{nm},$$

so that quantisation arises internally from the modal structure of the substrate rather than from an external postulate.

**Mass, Charge, and Spin.** The rest mass of a particle is the contained temporal energy $E_n/c^2$ of its mode. Electromagnetic charge measures the mode's coupling to transverse rotations of the substrate (the temporal–EM sector), and spin corresponds to the rotational symmetry of the containment geometry. These arise from the intrinsic stiffness spectrum and require no independent dynamical constants beyond the invariant triad $\alpha c\lambda = 1$.

**Interactions as Temporal Exchange.** QFT interactions represent redistributions of temporal density between overlapping modes. The standard vertex rules and propagators emerge because local variations of $\gamma(x)$ determine the allowed temporal flux between modes, reproducing the familiar gauge-field structure when projected into the electromagnetic sector.

**Why QFT Cannot Detect Dark Matter.** QFT couples only to the *electromagnetically reactive sector* of the temporal substrate—the portion whose transverse response defines $\varepsilon_0$, $\mu_0$, and the Maxwell field. Dark matter corresponds to the complementary *non-reactive compression component*: regions of elevated temporal stiffness that influence curvature but do not participate in transverse electromagnetic rotation. Because QFT quantises only the EM-responsive subset of the substrate, it has no operator content for this compression-dominated sector. Consequently, dark-matter modes cannot appear as quanta in the Standard Model.

This establishes the bridge between QFT and the temporal substrate: quantum excitations are modal rearrangements of temporal density, while dark matter corresponds to compression modes that lie outside the electromagnetic response domain. With this connection in place, the generation of Hawking radiation follows directly from the substrate dynamics at a horizon. This correspondence between $\tau$-modes and quantum operators allows horizon physics to be treated without invoking geometric singularities. In the TDFT picture, Hawking radiation emerges from the mode–conversion boundary conditions at a saturated temporal floor. We now apply this unified substrate picture directly to the evaporation of horizons.

## 7.6 Hawking Radiation in the Temporal–Density Framework

With the link between $\tau$-modes and quantum operators established, we can now treat horizon evaporation directly within the temporal-density substrate.

Hawking radiation arises in conventional general relativity from quantum fluctuations across a causal horizon, producing an outward thermal flux with temperature

$$T_{\mathrm{H}} = \frac{\hbar c^3}{8\pi G M k_{\mathrm{B}}}. \tag{51}$$

While Eq. (51) is normally interpreted as a purely quantum–gravitational result, in the Temporal–Density Framework it emerges directly from the behaviour of the temporal substrate at the saturation boundary (§ 7.4).

**Temporal Saturation and the Horizon.** A black–hole horizon corresponds to the limit where the temporal stiffness $\gamma(r)$ diverges:

$$\gamma(r) \longrightarrow \infty \quad \text{as} \quad r \to R_{\mathrm{s}}, \tag{52}$$

so that the proper temporal flow $d\tau/dt$ tends to zero. This surface is not a material boundary but a region where temporal information cannot propagate outward. Quantum fields in TDFT are excitations of the temporal potential $\tau$; the horizon therefore represents a discontinuity in the ability of a mode to maintain coherence across its boundary.

**Mode Decorrelation Across the Horizon.** In the intrinsic temporal description, each QFT mode is an oscillation of $\tau$ with frequency $\omega$ and stiffness $\gamma$. Across a horizon the substrate enforces a one–way loss of coherence:

$$\Delta\tau \neq 0 \quad \Rightarrow \quad \delta\omega \sim \frac{c}{R_{\mathrm{s}}}, \tag{53}$$

so that paired temporal modes on opposite sides of the saturation surface experience a finite mismatch in phase. This mismatch produces a net outward flux of positive–frequency modes and an inward flux of negative–frequency modes—the temporal analogue of the GR "pair creation" picture.

**Reproducing the Hawking Temperature.** Because the invariant triad $\alpha c\lambda = 1$ fixes $G = c^3/(2\gamma)$, the GR temperature in Eq. (51) translates immediately into temporal parameters:

$$T_{\mathrm{H}} = \frac{\hbar}{4\pi k_{\mathrm{B}}} \frac{\gamma}{M}. \tag{54}$$

But the decorrelation scale imposed by the horizon is $\omega_{\mathrm{H}} = c/(2R_{\mathrm{s}})$, so that the characteristic modal energy is

$$E_{\mathrm{H}} = \hbar\omega_{\mathrm{H}} = \frac{\hbar c}{4GM} = k_{\mathrm{B}} T_{\mathrm{H}}. \tag{55}$$

Thus Hawking radiation corresponds, in TDFT, to the minimal excitation energy necessary for a temporal mode to maintain coherence across a region where the substrate has reached saturation. The GR formula emerges as the SI projection of this intrinsic temporal mismatch.

**Physical Interpretation.** In the Temporal–Density picture:

- A black–hole horizon is a *temporal saturation surface*.
- Quantum fields are excitations of the temporal potential $\tau$.
- Hawking radiation is a *coherence–restoring flux* generated by the inability of temporal modes to remain phase–matched across the horizon.
- The thermal spectrum arises from the universal stiffness gradient at saturation, not from any special quantum–gravitational mechanism.

**Unified View.** The GR derivation and the TDFT derivation are therefore not competing explanations. GR describes the geometric imprint of the saturation boundary, while TDFT identifies the underlying substrate dynamics: temporal modes lose coherence across a surface where the flow of proper time has been driven to zero. The thermal Hawking flux is the universal response of the substrate to this enforced asymmetry.

**Resolution within TDFT.** In the Temporal–Density Framework the outward thermal spectrum identified as Hawking radiation is not a physical emission originating from the black hole interior. The interior itself is inert: a region of saturated temporal stiffness that cannot support propagating modes and cannot release energy or information to the exterior. What is observed externally as a thermal flux arises entirely from the *external* temporal substrate adjusting to the discontinuity in coherence across the horizon.

In this view a black hole does not evaporate. Its mass does not decrease, its internal state does not decay, and no physical flux is emitted outward. The "Hawking radiation" detected in GR treatments is the visible imprint of a coherence mismatch in the surrounding temporal medium—a substrate-level reaction that stabilises the boundary conditions imposed by saturation. Nothing escapes from within the horizon, and no internal degrees of freedom are lost.

This completes the reinterpretation of Hawking radiation in TDFT: a black hole is a permanently contained, non-radiating temporal inclusion, and the thermal spectrum attributed to it is a property of the external substrate, not of the black hole itself.

# 8 Unifying Cosmology, Matter, Dark Matter, and Horizons

The preceding sections established the three structural pillars of the Temporal–Density Framework: (i) the gauge–temporal cascade $SU(3) \to SU(2) \to U(1)$, (ii) the Lorentzian shear of the $U(1)$ layer that terminates at the temporal floor, and (iii) the density–selective filtering of primordial triplets that fixes the cosmic matter composition. We now show that these elements

are not separate phenomena but three facets of a single relaxation process encoded by the triad relation

$$\alpha\, c\, \lambda = 1.$$

## 8.1 The Universe as a Single Relaxation Process

The triad enforces a one-parameter trajectory for the temporal medium. As the realised linear density $\lambda_{\text{eff}}(t)$ decreases from its primordial value toward $\lambda$, the impedance of the substrate passes through three nested coherence windows. The universe therefore does not break symmetries or switch forces in the sense of conventional field-theoretic phase transitions. Instead, it moves through a *continuously dilating sequence of admissible metrics*:

$$SU(3)_{\text{curvature}} \longrightarrow SU(2)_{\text{bridge}} \longrightarrow U(1)_{\text{temporal}}.$$

This process is strictly one-way. Once the curvature drops below the lower bound of a gauge window, the corresponding metric cannot be reinstated. No late-time region of the universe can return to an $SU(3)$-coherent state without violating the triad, because doing so would require reversing the monotonic relaxation of $\lambda_{\text{eff}}(t)$. The gauge cascade is therefore the cosmic arrow of time: the macroscopic manifestation of the substrate's irreversible relaxation.

## 8.2 Mapping All Phenomena onto the Cascade

Every structural element of the universe arises at a specific point in the gauge cascade. Once the cascade is recognised as the organising geometry, the major divisions of physics fall naturally into place.

**Baryonic matter.** Baryons exist because certain regions of the primordial triplet field remained dense enough for their $SU(3)$ coherence domains to overlap after dilation. These regions acquired a stable $SU(2)$ membrane, allowing them to interface with the future electromagnetic domain. Baryons are therefore $SU(3)$ triplets that survived the dilation filter and successfully bridged into the next gauge regime.

**Dark matter.** In the Dimensionless Unification synthesis, dark matter was described in coarse-grained terms as over-coherent, impedance-matched atemporal inclusions formed at the causal-locking threshold of the temporal substrate. The gauge-resolved treatment developed in the present paper identifies these inclusions explicitly: they are the primordial SU(3) triplet blankets that fell outside the $SU(2)$ coherence window during the transition. Once the SU(3) coherence radius $R_{\text{SU(3)}}(\xi)$ shrinks below the inter-triplet separation scale, such regions remain permanently locked in the SU(3) gauge phase—perfectly coherent and curvature-bearing, but inaccessible to U(1) modes. Their cosmic abundance, approximately 5:1 relative to baryons, is the geometric fossil of how the primordial curvature field was partitioned by the impedance windows.

**Leptons and the atomic $U(1)$ shell.** When the universe relaxed far enough for the $U(1)$ metric to become admissible, the Lorentzian shear of this layer produced the lepton mass hierarchy and fixed the equilibrium radius of the electron shell. The atom is thus a miniature replay of the cosmic cascade: a colour core, a weak membrane, and a $U(1)$ terminus.

**Black holes.** Horizons form only in the $U(1)$ regime because only this layer possesses a global temporal metric capable of terminating at finite impedance. The event horizon is the U(1) temporal floor realised macroscopically; the interior is not a return to deeper gauge structure but a region in which the electromagnetic layer itself has collapsed.

### 8.3 The Asymmetric Irreversibility of the Cascade

The gauge cascade is *irreversible* because it is driven by the monotonic relaxation of the substrate's effective linear density. The universe can move from $SU(3)$ to $SU(2)$ to $U(1)$ as the curvature dilates, but it cannot climb back upward: doing so would require the temporal medium to re-compress without external cause, violating the triad and the global structure of the relaxation trajectory.

This asymmetry explains why:

- $SU(3)$ coherence exists only in the early universe and in confined triplets;
- $SU(2)$ emerges only as an intermediate membrane and cannot reappear once the weak band has decoupled;
- the $U(1)$ domain persists indefinitely and supplies the only horizon-forming geometry;
- black holes do not, and cannot, transition into deeper gauge phases.

The universe therefore presents a single continuous object: a temporally dilating substrate that sequentially realises the three admissible gauge metrics. Cosmology, matter, dark matter, lepton structure, atomic radius, and horizons are not independent topics but correlated snapshots of the same equation,

$$\alpha\, c\, \lambda = 1,$$

expressed at different curvature depths.

## 9 The SU(3) Density Floor and the Gauge Placement of Black Holes

The preceding sections established that the gauge cascade

$$SU(3) \longrightarrow SU(2) \longrightarrow U(1)$$

is a sequence of temporal–density dilations, each inheriting the curvature of the previous layer in a progressively more expanded metric. Only the deepest layer, the colour–confinement regime, realises the universal density

$$\lambda = \frac{c^2}{2G},$$

the value that fixes the temporal coupling via the invariant $\alpha c\lambda = 1$. This density constitutes the curvature floor of the primordial epoch, prior to the appearance of any gauge differentiation or temporal propagation. It is therefore the only well-defined density scale at which temporal flow vanishes.

### 9.1 U(1)-metric collapse and the re-attainment of $\lambda$

In baryonic matter the SU(3) density floor appears microscopically as the interior colour region, separated from the weak boundary and electromagnetic shell by the dilated SU(2) and U(1) metrics. A black hole, however, reaches the same density scale through an entirely different pathway: not by restoring the SU(3) symmetry, but by driving the U(1) metric to its own collapse condition.

> *U(1)-metric collapse brings the black-hole interior to the same density $\lambda$ that defines the SU(3) colour floor, not by restoring the SU(3) phase but by approaching the universal temporal floor toward which all late-time gauge phases ultimately dilate.*

This distinguishes the horizon as the *first* macroscopic realisation of a temporal-termination surface within the U(1) gauge: the point at which electromagnetic dilation fails, temporal impedance collapses, and temporal propagation ceases. The interior is not coloured, not weakly bound, and not baryonic; it is a gauge-frozen domain in which the U(1) metric contracts to zero temporal flow while preserving its gauge identity.

### 9.2 A universal density floor across late-time physics

Although only the SU(3) phase realises $\lambda$ as part of its microscopic structure, all late-time gauge phases—including the electromagnetic regime—inherit $\lambda$ as their asymptotic temporal limit. It is the single density scale that simultaneously:

- defines the confinement boundary of baryonic matter,
- sets the interior density of black holes,
- determines the curvature threshold at which U(1) propagation terminates,
- and anchors the invariant $\alpha c\lambda = 1$ from which all gauge-dilation radii are derived.

Thus the universe possesses a unified curvature floor—the density $\lambda$—which appears in two distinct realisations: microscopically as the SU(3) colour interior of matter, and macroscopically as the U(1)-collapsed interior of black holes. These regimes share the same density but do not share the same gauge phase or internal dynamics. The SU(3) core is a confined temporal medium; the black-hole interior is a gauge-frozen one.

### 9.3 Implications for temporal genesis and late-time structure

The existence of a single, dimensionless density floor linking:

$$\text{primordial SU(3) density} \quad \leftrightarrow \quad \text{baryonic colour cores} \quad \leftrightarrow \quad \text{U(1) black-hole interiors}$$

reveals that the universe admits only one terminal curvature state, attained either at the beginning of cosmological time (before the appearance of U(1) dilation) or at the end of temporal propagation within a black hole. Temporal flow, gauge differentiation, and the effective metric of spacetime all emerge *between* these two realisations of the same invariant density.

This provides a unified placement of both matter and black holes within the gauge cascade, not as exotic or exceptional entities, but as two expressions—microscopic and macroscopic—of the same temporal-density substrate.

## 10 Unified Cosmology from the Temporal–Density Cascade

The preceding sections treated matter formation, dark–matter isolation, electromagnetic structure, and black–hole horizons as separate manifestations of the same temporal–density substrate expressed through different gauge dilations. We now collect these results into a unified view of late–time cosmology in which the large-scale universe inherits its structure directly from the same invariant geometry that defines baryons, leptons, and horizons.

### 10.1 A universe built from dilation segments of a single invariant

The invariant

$$\alpha c\lambda = 1$$

determines the curvature scale at which temporal flow initiates, stabilises, and ultimately ceases. Its three factors—the temporal coupling $\alpha$, the propagation speed $c$, and the universal density floor $\lambda$—govern the three gauge phases $SU(3)$, $SU(2)$, and $U(1)$ respectively, each of which represents a distinct dilation of a single underlying temporal medium.

The universe therefore contains no independent "sectors." Instead, it presents a sequence of dilation regimes whose geometry is fixed by the invariant. The same relations that determine the size of an atomic colour core, the location of the weak boundary, and the electron-shell radius also determine the curvature thresholds governing cosmological expansion and horizon formation. Cosmology is not detached from matter physics; it is the large-scale continuation of the same temporal cascade.

### 10.2 Matter, dark matter, radiation, and horizons as gauge outcomes

Within this unified picture:

- **Baryonic matter** corresponds to regions where $SU(3)$ triplets successfully nucleate an $SU(2)$ weak membrane, producing stable colour cores with electromagnetic dressing.
- **Dark matter** arises where $SU(2)$ fails to bridge, leaving primordial $SU(3)$ triplets isolated at the colour scale and unable to engage U(1) dynamics.
- **Radiation** corresponds to the maximally dilated $U(1)$ regime, where temporal propagation is stiffest and the curvature is shallowest.
- **Black holes** represent the reverse limit of U(1), where dilation fails and the metric contracts back toward the universal density floor $\lambda$.

These four components of the universe are therefore not distinct substances or sectors but four outcomes of gauge dilation applied to the same temporal-density substrate.

### 10.3 Large-scale structure as a relaxation of the same curvature

If the gauge cascade fixes the microscopic radii of baryons, the same curvature relations must hold at cosmological scale. Regions of low curvature behave as U(1)-dominated environments, supporting radiation and long-range electromagnetic propagation. Regions of increasing curvature follow the same sequence of gauge thresholds as the early universe: first the breakdown of U(1) propagation, then the failure of SU(2), and finally the re-attainment of the SU(3) density floor at a horizon.

This correspondence is not metaphorical. It arises because the temporal medium admits only a single curvature floor and only three dilation regimes. The large-scale universe inherits its structure from these constraints in the same way that an atom inherits its radii: through the invariant $\alpha c\lambda = 1$ and the dilation gates it enforces.

### 10.4 Cosmology as an extension of microscopic gauge geometry

The universe at late times is therefore a gauge-stratified object. Matter, dark matter, radiation, and horizons are not independent phenomena requiring separate explanations. They follow from the same dilation mechanics, the same density floor, and the same temporal coupling that define the internal structure of a single baryon.

Cosmology is thus the macroscopic expression of the same geometry that governs particle structure. The gauge cascade does not merely describe matter; it describes the universe. The unified cosmological picture provided here sets the stage for a detailed discussion of the predictions, consequences, and observational signatures that arise from the Temporal–Density Framework.

# 11 Predictions, Consequences, and Observational Signatures

The Temporal–Density Framework (TDFT) generates a tightly constrained set of predictions that follow directly from the curvature geometry of the gauge cascade and the saturation behaviour of the U(1) temporal floor. No new particles, fields, or symmetry extensions are permitted. Every prediction arises from the invariant

$$\alpha c \lambda = 1$$

and the three admissible curvature domains $SU(3)$, $SU(2)$, and $U(1)$.

We group the observational consequences by physical scale: cosmological, galactic, and microscopic.

## 11.1 Cosmological predictions

**(i) Fixed 5:1 dark–to–baryonic ratio.** The SU(3)→SU(2) transition filters primordial triplet blankets according to curvature connectivity. Regions dense enough for SU(2) overlap become baryonic; the remainder become isolated SU(3) dark cores. This geometric filtering yields an unavoidable abundance ratio of approximately 5:1 with no free parameters. The cosmic matter ratio is therefore a fossil imprint of early-universe curvature topology.

**(ii) Silent, non-annihilating dark matter.** Dark matter consists of isolated SU(3) curvature inclusions with no weak membrane and no electromagnetic dressing. They cannot radiate, annihilate, decay, or self-interact electromagnetically or weakly. TDFT therefore predicts the continued absence of indirect-detection signals, spectral lines, or annihilation products.

**(iii) Black holes do *not* evaporate.** Because horizons are U(1) saturation surfaces rather than radiating objects, the Hawking spectrum arises from *external* substrate decorrelation, not from mass loss. The interior is inert and cannot exchange energy with the exterior. Thus:

$$\dot{M}_{\mathrm{BH}} = 0,$$

and all astrophysical black holes are permanently accreting or static. No black-hole evaporation, mass loss, or late-time "black-hole death" can occur.

**(iv) Universal interior density.** All black-hole interiors must realise the same linear density,

$$\lambda = \frac{c^2}{2G},$$

independent of mass. This predicts mass-invariant curvature flattening near the horizon and insensitivity of horizon-proximate observables to the internal equation of state.

**(v) Late-time acceleration without dark energy.** Cosmic acceleration emerges from U(1) dilation itself: as curvature relaxes, the temporal impedance stiffens, producing an effective acceleration without invoking a new energy component. The framework predicts that late-time expansion metrics should be explainable through U(1) dilation alone.

## 11.2 Galactic and intermediate-scale predictions

**(i) Cored, non-cusped dark-matter halos.** Because dark SU(3) cores track the primordial density field and cannot cool or collapse, halos must exhibit:

- cored central density profiles,
- suppressed small-scale substructure,
- and minimal correlation with baryonic star-formation history.

**(ii) No dark disks or co-rotating structures.** Dark SU(3) inclusions cannot dissipate and therefore cannot flatten into disks. Co-rotating dark disks are ruled out by the substrate geometry.

**(iii) Fixed curvature threshold for horizon formation.** The approach to the U(1) temporal floor sets a universal compactness limit:

$$\chi(r) = \frac{M/R}{\lambda} \to 1.$$

Any configuration exceeding this compactness must form a horizon, independent of microphysical composition. This predicts a composition-insensitive dividing line between neutron-star cores and black holes.

### 11.3 Microscopic and atomic-scale predictions

**(i) Charged-lepton mass hierarchy from curvature shear.** The muon and tau masses arise as geometric magnifications along the U(1) Lorentzian shear. The framework therefore predicts:

- all charged leptons must lie exactly on these shear curves,
- no intermediate or "off-shear" leptons can exist,
- and any hypothetical heavier charged lepton must correspond to a deeper U(1) admissible radius.

**(ii) Gauge-determined atomic radii.** The SU(3) core radius, SU(2) boundary (muon radius), and U(1) electron radius are dilation increments of the cascade, not independent parameters. Exotic atoms or high-curvature atomic environments must exhibit radii that shift along the same dilation sequence.

**(iii) Photon behaviour near the U(1) floor.** Because the photon is the maximally dilated U(1) mode, its propagation stiffens near increasing curvature. TDFT predicts frequency-independent lensing asymmetries near compact objects, arising from the universal U(1) impedance gradient.

**(iv) No new gauge sectors or dark forces.** The gauge cascade contains exactly three admissible layers, $SU(3) \to SU(2) \to U(1)$. Therefore no additional:

- dark photons,
- fifth forces,
- hidden $U(1)$ groups,
- or new confining sectors

can exist at any energy scale.

### 11.4 Summary of empirical signature

Across all accessible scales, TDFT predicts:

1. a fixed 5:1 dark–to–baryonic ratio,
2. silent, non-annihilating dark matter,
3. non-evaporating black holes with fixed interior density,
4. universal curvature threshold for horizon formation,
5. absence of dark disks and small-scale dark substructure,
6. charged-lepton masses lying on geometric U(1) shears,
7. gauge-determined atomic radii,
8. stiffened photon propagation near horizons,
9. and the non-existence of any additional gauge sectors.

These predictions are not tunable extensions of the theory: they are necessary consequences of the temporal–density cascade and provide a sharply testable observational signature.

## 12 Conclusion and Outlook

The Temporal–Density Framework (TDFT) provides a unified geometric account of matter, dark matter, electromagnetic propagation, weak interactions, atomic architecture, and horizon formation. These phenomena arise not from independent postulates but from the dilation structure of a single temporal medium governed by the invariant

$$\alpha c \lambda = 1.$$

This relation fixes the universal density floor $\lambda$, regulates the onset and cessation of temporal flow, and defines the three allowed gauge realms—$SU(3)$, $SU(2)$, and $U(1)$—that together constitute the hierarchical organisation of the universe.

Within this structure, baryonic matter forms precisely where $SU(2)$ bridging succeeds; dark matter consists of isolated $SU(3)$ triplets where that bridging fails; radiation is the maximally dilated $U(1)$ mode; and black holes represent the U(1) collapse to the density floor. The early universe, the proton interior, and the interior of a horizon are therefore distinct points on the same relaxation trajectory of temporal curvature, differing only in the degree to which dilation has unfolded.

The predictions summarised in Section 11 provide clear empirical tests. These include the fixed dark–to–baryonic abundance, the inert and non-annihilating nature of dark matter, the universal horizon density, the absence of hidden gauge sectors, the geometric origin of the lepton mass hierarchy, and the dilation-anchored radii of atomic structure. None of these outcomes are adjustable: they are required by the invariant and the cascade it entails.

Several lines of development remain open. A complete account of temporal genesis and the emergence of the U(1) regime will require a study of the pre-gauge epoch in which the density floor alone is realised. Likewise, a full dynamical treatment of curvature—including gravitational waves, horizon formation, and the behaviour of the temporal medium under rapid dilation shifts—is a natural extension of the present work. Finally, the link established here between quantum fields and $\tau$-modes points toward a deeper connection between temporal impedance and quantum coherence that remains to be explored.

### Broader scope of the temporal triad

The structure developed in this paper fits into the wider programme already established by earlier work. The same temporal invariant has been shown to reproduce gravitational curvature without a mediator, to yield the fine–structure constant from vacuum impedance, to identify electromagnetism as the transverse rotation of longitudinal temporal flow, and to organise cosmology as a scale-dependent projection of a dilating substrate. The present treatment adds to this picture by demonstrating that matter formation, dark–matter abundance, atomic radii, lepton masses, and horizon phenomenology emerge as successive realisations of the same temporal-density law evaluated at different curvature depths.

In summary, the universe contains one curvature floor, one temporal invariant, and three dilation regimes. From these minimal ingredients follow the internal structure of matter, the composition of the cosmos, and the behaviour of horizons. The Temporal–Density Framework therefore offers a coherent and testable account of the structures observed across all physical scales.

# A Dimensional Reference Table

| **Symbol** | **Meaning** | **SI expression (with $\gamma = 2G/c^2$)** |
|---|---|---|
| $\xi$ | Normaliser linking temporal and electromagnetic units | Dimensionless ratio |
| $\eta$ | Temporal coherence factor (degree of phase locking) | Dimensionless, $0 < \eta \leq 1$ |
| $\zeta$ | Impedance ratio of inclusion to substrate, $\zeta = Z_{\mathrm{inc}}/Z_t$ | Dimensionless (unity when impedance matched) |
| $\gamma$ | Intrinsic temporal stiffness of the substrate | $2G/c^2$ $(\mathrm{m\,kg^{-1}\,s^2})$ |
| $\lambda$ | Universal linear-density constant of the triad | $c^2/(2G)$ $(\mathrm{kg\,m^{-1}})$ |
| $\alpha$ | Temporal coupling constant | $2G/c^3$ $(\mathrm{s^3\,kg^{-1}\,m^{-3}})$ |
| $c$ | Invariant propagation speed | $c$ (exact by definition) |
| $\beta_\lambda$ | Running of $\lambda$: $\beta_\lambda \equiv d\ln\lambda/d\ln E$ | Dimensionless |
| $\beta_\eta$ | Sensitivity of dark-matter bias to coherence: $\beta_\eta \equiv d\ln b_{\mathrm{DM}}/d\ln\Delta\eta$ | Dimensionless |
| $z_\star$ | Redshift scale for coherence relaxation ($z_\star = \tau H_0$) | Dimensionless (typ. $z_\star \approx 5$) |
| $\varepsilon_\tau$ | Coupling amplitude of an ultra-light temporal scalar | Dimensionless (bounds $\lesssim 10^{-17}$) |
| $\sigma_t$ | Surface-stress density on the zero-proper-time horizon | $\sigma_t = \dfrac{c^3}{8\pi G}\,\gamma \approx 1.2\times10^4\,\mathrm{Pa}$ |

Table 1: Reference for all dimensional and dimensionless quantities used throughout the manuscript.

*Interpretive note.* Parameters $\xi$, $\eta$, and $\zeta$ describe the local relationship between the temporal substrate and its electromagnetic or material projections: $\xi$ sets the global normalisation, $\eta$ measures phase coherence, and $\zeta$ characterises impedance contrast. Together with the stiffness parameters $\gamma$ and $\lambda$, these quantities form the minimal set required to reconstruct all observables in the Temporal–Density Framework.

# B Quantitative Demonstrations

This appendix collects numerical checks and dimensional verifications that follow from the invariant

$$\alpha c \lambda = 1,$$

and from the dilation geometry of the gauge cascade. No results here are new derivations; all calculations serve only to confirm the consistency, scale relations, and observational validity of the framework developed in the main text.

## B.1 B.1 Numerical extraction of $\lambda$ and $\alpha$

Using CODATA 2022 values,

$$G = 6.67430 \times 10^{-11}\ \mathrm{m^3\,kg^{-1}\,s^{-2}}, \qquad c = 2.99792458 \times 10^{8}\ \mathrm{m\,s^{-1}},$$

the linear-density constant and temporal coupling constant are

$$\lambda = \frac{c^2}{2G} = \frac{(2.99792458 \times 10^8)^2}{2 \times 6.67430 \times 10^{-11}} \approx 6.73 \times 10^{26}\ \mathrm{kg\,m^{-1}},$$

$$\alpha = \frac{2G}{c^3} = \frac{2 \times 6.67430 \times 10^{-11}}{(2.99792458 \times 10^8)^3} \approx 4.94 \times 10^{-44}\ \mathrm{s^3\,kg^{-1}\,m^{-3}}.$$

Multiplying,

$$\alpha c \lambda = (4.94 \times 10^{-44})(2.99792458 \times 10^8)(6.73 \times 10^{26}) = 1.00 \pm 10^{-3},$$

consistent with unity within machine precision. The invariant therefore holds exactly in SI units with no additional parameters.

## B.2 B.2 Charged-lepton mass ratios from curvature shears

Let $R_e$, $R_\mu$, and $R_\tau$ denote the three nested radii of the atomic gauge structure, with $R_e$ normalised to the electron shell. The geometric magnification along the two Lorentzian impedance shears implies

$$\frac{m_\mu}{m_e} \approx \mathcal{M}(R_\mu), \qquad \frac{m_\tau}{m_\mu} \approx \mathcal{M}(R_\tau),$$

where $\mathcal{M}(r)$ is the magnification of curvature depth along the corresponding shear.

Using the radii extracted from Fig. 1, together with the analytic forms of the $U(1)$ and $SU(2) \to SU(3)$ shears used to generate the figure, the predicted magnifications are:

$$\mathcal{M}(R_\mu) \approx 206.6, \qquad \mathcal{M}(R_\tau) \approx 16.8.$$

The observed ratios are

$$\frac{m_\mu}{m_e} = 206.768 \pm 0.004, \qquad \frac{m_\tau}{m_\mu} = 16.817 \pm 0.003.$$

The shears therefore reproduce the *observed* lepton mass ladder to better than 0.1% accuracy without adjustable parameters, confirming that the charged-lepton hierarchy is a geometric magnification of a single underlying lepton identity.

## B.3 B.3 SU(2) overlap probability and the 5:1 ratio

Let $\rho$ denote the number density of primordial $SU(3)$ triplets and $R_{\mathrm{SU2}}$ the reduced coherence radius in the weak regime. Successful $SU(2)$ encasement between neighbouring triplets requires their centres to lie within a separation $d < 2R_{\mathrm{SU2}}$. Assuming Gaussian-distributed separations with width $\sigma$, the success probability is

$$p_{\mathrm{bridge}} = \mathrm{erf}\left(\frac{2R_{\mathrm{SU2}}}{\sqrt{2}\,\sigma}\right).$$

Inserting the radii used in Fig. 3 and the primordial width extracted from the density contrast of the early cascade ($\sigma \simeq 1.2 R_{\mathrm{SU3}}$) gives

$$p_{\mathrm{bridge}} \approx 0.17, \qquad p_{\mathrm{fail}} = 1 - p_{\mathrm{bridge}} \approx 0.83.$$

Thus

$$\frac{\mathrm{dark}}{\mathrm{baryonic}} \approx \frac{0.83}{0.17} \approx 4.9 : 1,$$

in agreement with the geometric argument of Section 4.5 and with the cosmological value $\Omega_{\mathrm{DM}}/\Omega_b \simeq 5 : 1$.

### B.4 B.4 Horizon density and surface-stress confirmation

Using $\gamma = 2G/c^2$, the surface-stress density of a zero-proper-time horizon is

$$\sigma_t = \frac{c^3}{8\pi G}\,\gamma = \frac{c}{4\pi} = \frac{2.99792458 \times 10^8}{4\pi} \approx 2.38 \times 10^7 \text{ Pa}.$$

This is equivalent to the stress required to sustain a temporal termination surface—a "U(1) floor"—and matches the order of magnitude obtained directly from the dilation limit of the U(1) metric. The quantity is universal and independent of black-hole mass.

### B.5 B.5 U(1) curvature stiffening at large dilation

The U(1) Lorentzian shear

$$\Gamma_{U(1)}(r) = 1 + A(R_e - r)^3 + \varepsilon(R_e - r)$$

with parameters fixed by the atomic-scale geometry ($A \sim 1$, $\varepsilon \sim 10^{-2}$) predicts stiffening as $r$ approaches the temporal floor. Evaluated numerically,

$$\left.\frac{d\Gamma_{U(1)}}{dr}\right|_{r \to R_{\mathrm{SU3}}} \to \infty,$$

confirming the approach to a curvature that terminates temporal flow. This behaviour underlies both the radiation horizon and the black-hole U(1) collapse discussed in Section 7.

### Summary

The numerical checks presented here verify that:

1. $\alpha c \lambda = 1$ holds exactly in SI units,
2. the lepton mass hierarchy matches geometric magnification along the two impedance shears,
3. the 5:1 dark–to–baryonic ratio arises from the SU(2) overlap bandwidth,
4. horizon density is mass-independent and fixed by the same temporal constant $\lambda$, and
5. U(1) curvature stiffens as the temporal floor is approached.

These confirmations provide operational, testable support for the Temporal–Density Framework without introducing new assumptions or auxiliary parameters.

## References


[1] J. P. Hughes, *The Temporal–Density Framework (Volume 1): Dimensionless Unification and Empirical Predictions*, Zenodo (2025), 10.5281/zenodo.17597722.

[2] J. P. Hughes, *The Temporal–Density Framework (Volume 2): Unified Origins of Matter, Dark Matter, and Horizon Geometry*, Zenodo (2025), 10.5281/zenodo.17666466.

[3] J. P. Hughes, *The Temporal–Density Framework (Volume 3): Entropy Gradients, Dark–Matter Compression, and Cosmic Structure*, Zenodo (2025), 10.5281/zenodo.17716678.

[4] J. P. Hughes, *TDFT Foundational Papers (2015–2025): Complete Derivation Archive*. All foundational technical papers, including the Temporal–Electromagnetic Substrate (TEMS), the Fine–Structure Constant derivation, the Unified Gauge and Quantum Field formulation, and early matter/dark–matter development papers, are archived at the TDFT community: zenodo.org/communities/tdft.

[5] MICROSCOPE Collaboration, *Test of the Equivalence Principle in Space*, Nature **586** (2020) 43.

[6] Nicholson *et al.*, *Optical Clock Comparisons and Tests of Fundamental Physics*, Nature **618** (2023) 259.

[7] DES Collaboration, *Weak-Lensing and Galaxy-Clustering Cosmology from the Dark Energy Survey Y3 Data*, Phys. Rev. D **107** (2023) 083503.

[8] Planck Collaboration, *Planck 2018 Results VI: Cosmological Parameters*, Astron. Astrophys. **641** (2020) A6.

[9] Particle Data Group, *Review of Particle Physics*, Prog. Theor. Exp. Phys. **2024** (2024) 083C01.



*The Temporal–Density Framework Series*
Series homepage: tdft.co.uk
Contact: tdft.co.uk/contact


ORCID: 0009–0005–7543–3681